

Experimental Study of Laser-Compton Scattering in the Non-linear Regime

Y.Kamiya*, T.Kumita

Department of Physics, Tokyo Metropolitan University, Japan

I.Ben-zvi, K.Kusche, I.Pogorelsky, P.Siddons, V.Yakimenko
Brookhaven National Laboratory, USA

T.Omori, J.Urakawa, K.Yokoya

High Energy Accelerator Research Organization, Japan

T.Hirose, S.Kashiwagi, M.Washio

Advanced Research Institute for Science and Engineering, Waseda University, Japan

D.Cline, and F.Zhou

University of California, Los Angeles, USA

Abstract

We have performed experiments for generating high brightness X-ray beam via Compton scattering of 60 MeV electron and high power CO₂ laser beams at Brookhaven National Laboratory. In the near future, the CO₂ laser system will be upgraded to provide 1 TW peak power and it enables us to observe Compton scattering in the nonlinear regime. For measurement of the X-ray energy spectrum and angular distribution from the nonlinear Compton scattering, we designed an X-ray spectrograph consists of a multilayer crystal and a two-dimensional position sensitive detector.

1 INTRODUCTION

Development of high-intensity, short-pulse, and compact X-ray sources is required for various fields of scientific, industrial, and medical applications. One of the most promising methods for producing such an X-ray beam is known as Laser Synchrotron Source (LSS), which utilizes laser-Compton scattering (inverse Compton scattering) via interaction between high-power pulsed laser and electron beams [1].

We have performed a series of laser-Compton experiments since 1998 using a high power CO₂ laser and a 60 MeV electron beam provided at the Brookhaven Accelerator Test Facility (BNL-ATF). We demonstrated production of 2.5×10^7 X-ray photons/pulse with the pulse duration of 3.5 psec for 600 MW CO₂ power in 1999 [2][3], and 1.7×10^8 X-ray photons/pulse for 14 GW CO₂ power in 2001 [4]. In the near future, the CO₂ laser system will be upgraded to provide 1 TW peak power. We expect to observe nonlinear Compton scattering of the electron and laser beams in that stage. Until now, two observations of nonlinear Compton scattering were carried out for scattered photons in visible and γ -ray region [5][6] by measuring energy of the scattered photons or the recoiled electrons.

We propose a new technique to observe a laser-Compton scattering in the nonlinear regime by measuring angular distribution and energy spectrum of the scattered photons simultaneously. In this report, we describe details of the experimental plan, simulation study and design of the detector.

2 EXPERIMENTAL APPARATUS

The experimental apparatus located at the BNL-ATF consists of three major components, a 60MeV electron linac, a CO₂ laser system, and an Nd:YAG laser system. The electron beam is generated by the laser photo-cathode RF gun and accelerated to 60 MeV by the S-band linac, and then supplied to three extraction lines in the experimental hall. The CO₂ laser system is located outside the experimental hall separated with a radiation shielding wall. The laser beam is amplified by a pre-amplifier and a main-amplifier, and then transported to the experimental hall. Typical parameters of the electron beam and the CO₂ laser are shown in Table 1.

Table 1: Parameters of the electron beam and the CO₂ laser beam

Electron beam	
Beam energy	60 MeV
Bunch charge	0.5 nC
Bunch length (FWHM)	3.5 ps
Beam size at focus point (σ_x/σ_y)	32/32 μm
CO₂ laser (after upgrade)	
Wavelength	10.6 μm
Pulse energy	3 J/pulse
Pulse length (FWHM)	3 ps
Beam size at focus point (σ_x/σ_y)	32/32 μm
Normalized Vector potential	0.77

*E-mail: kamiya-yoshio@phys.metro-u.ac.jp

The Nd:YAG laser pulse is divided for the laser photocathode RF gun and for optical switch of the CO₂ laser system placed between the oscillator and the pre-amplifier. An adjustable optical delay is placed between the Nd:YAG laser and the optical switch. This system allows us to adjust coincidence of the CO₂ laser and electron beams within sub-picoseconds and thus the BNL-ATF is one of the best places for studying interactions between high power laser and electron beams, such as the Compton scattering experiment.

The interaction chamber (Compton cell) is set to the first extraction line of the BNL-ATF linac. Fig. 1 shows the principle setup of the experiment. The CO₂ laser beam is focused onto the center of the Compton cell with a parabolic copper mirror, which has a 5 mm diameter hole along the beam axis to allow the electron beam and produced X-ray beam to go through. This design of the Compton cell enables head-on collision of the CO₂ laser and electron beams, the most efficient collision in terms of intensity of produced X-rays via Compton scattering.

X-rays generated at the center of the Compton cell are transmitted through the hole of the mirror, and extracted to the air through a beryllium (Be) window with 250 μm thickness placed 1 m downstream from the interaction point for vacuum seal. A silicon (Si) photodiode was used for X-ray detection in the previous runs. A new detection system called X-ray spectrograph will be installed for measurement of energy spectrum in the next run. Details of the spectrograph are described in Section 4.

3 NONLINEAR COMPTON SCATTERING

Magnitude of the nonlinear Compton scattering is characterized by the normalized vector potential;

$$a = \frac{e}{m_e c^2} \sqrt{-\langle A_\mu A^\mu \rangle},^1 \quad (1)$$

where e is charge of the electron, A_μ is four-vector potential of the laser, and $m_e c^2$ is electron's rest energy. It can be written in more convenient form as a function of wavelength λ and power density I of the laser for circular polarization as follows;

$$a = 0.60 \times 10^{-9} \cdot \lambda[\mu\text{m}] \cdot I^{1/2}[\text{W}/\text{cm}^2]. \quad (2)$$

Compton scattering occurs in the linear regime for $a \ll 1$, while the nonlinear Compton scattering is comparable to the linear process for $a \simeq 1$.

The normalized vector potential of the CO₂ laser after planned upgrade is expected to be $a = 0.77$. To study the nonlinear Compton scattering in the future runs, energy spectrum and angular distributions of X-rays are simulated by an MC simulation code, CAIN [7], which describe the interactions between electrons, positrons, photons and high power electromagnetic field. Fig. 2 shows the result of the

simulation. The solid line shows the energy spectrum of generated X-rays for the upgraded laser ($a = 0.77$), while the dashed line shows that for the previous run in 2001 ($a = 0.04$). In comparison with the dashed line, the solid line has a smooth shoulder due to an electron mass shift in the laser field and higher energy photons are seen due to the higher order interactions.

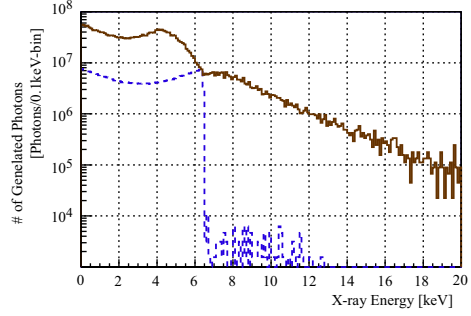


Figure 2: Energy spectra of Compton X-rays for laser power at the present stage, $a = 0.04$ (dash line) and after planned upgrade, $a = 0.77$ (solid line). They are simulated by CAIN [7] with the parameters shown in Table 1

Fig. 3 shows energy and angular distributions of the X-rays in the non-linear regime ($a = 0.77$). The x-axis shows the energy in keV, while the y-axis shows the scattered angle, θ , in mrad. The bands appeared in the plot correspond to the 1st harmonic, 2nd harmonic, 3rd harmonic and so on from the left hand side. The effect of the mass shift appears as width of each band in the plot. Therefore, order of the interaction is identified by measuring energy and scattered angle of the X-ray photons simultaneously. We design the X-ray spectrograph sensitive in the energy-angular range surrounded with the square in Fig. 3 for this purpose.

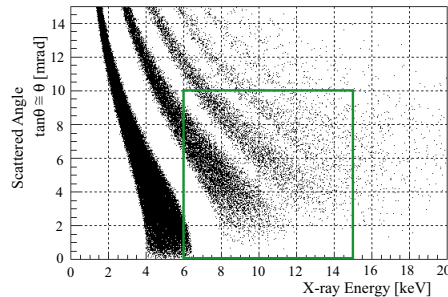


Figure 3: Scatter plot of energy and angular distributions of X-ray photons simulated by CAIN for circularly polarized laser beam of $a = 0.77$. The bands appeared in the plot correspond to the 1st, 2nd, 3rd harmonics from the lhs. The square shows acceptance of the detector system (See section 4)

¹ $A_\mu A^\mu \equiv A_0^2 - \mathbf{A}^2$

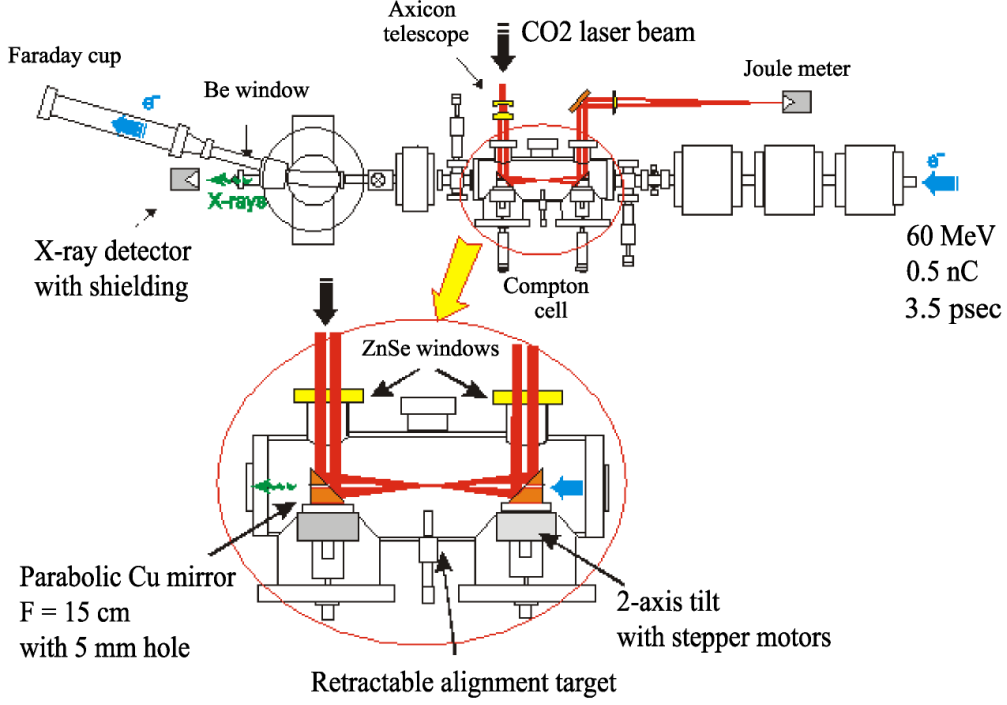


Figure 1: Experimental setup around the collision point.

4 X-RAY SPECTROGRAPH

The X-ray spectrograph, designed for observation of nonlinear Compton scattering, consists of a Silicon/Molybdenum (Si/Mo) multilayer crystal, and a two-dimensional position sensitive detector.

The multilayer crystal has 45-pair periodic structure with thickness of each layer 20 Å. It reflects X-rays as a natural single crystal with the lattice spacing of 40 Å does. Relation between the reflection angle and X-ray energy is given by the Bragg's law;

$$\sin \theta_B = n \cdot \frac{0.155}{E_{X\text{-ray}} [\text{keV}]}, \quad (3)$$

where θ_B is the Bragg angle for the energy, $E_{X\text{-ray}}$, and n is an order of diffraction.

The multilayer crystal is curved cylindrically as shown in Fig. 4. The curvature makes incident angle of X-rays to the multilayer crystal vary from 25 mrad to 10 mrad, corresponding to the X-ray energy satisfies the Bragg's law from 6 keV to 15 keV. Thus energy spectrum of X-rays appears as angular distribution along the X-axis in Fig. 4. On the other hand, reflection angle along the Y-axis directly represents emission angle of X-ray from the collision point. Therefore, energy and emission angle of X-rays are measured simultaneously by detecting reflected X-rays using a two-dimensional detector.

We use a CCD based X-ray detector (MarCCD X-ray detector, Mar USA Inc.) for two-dimensional detection. It consists of a scintillation screen with 162 mm diameter,

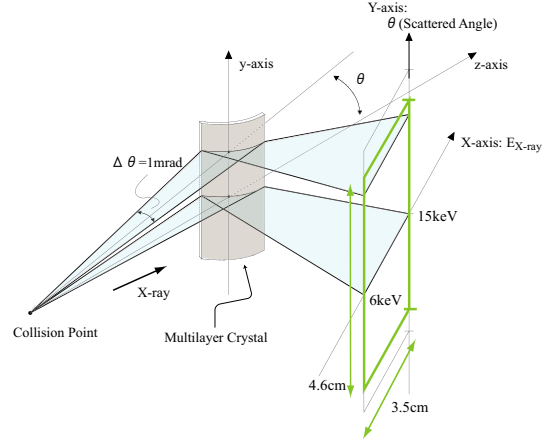


Figure 4: A schematic view of the X-ray spectrograph.

a fiber optic taper which guides scintillation lights, and a CCD detector. The CCD has $2k \times 2k$ pixels and each pixel provides a 16-bit readout. The pixel size corresponds to a $80 \mu\text{m} \times 80 \mu\text{m}$ square on the scintillation screen.

Fig. 5 shows a simulation image obtained on the CCD detector. The X-ray photons are generated by CAIN for $a = 0.77$ and then traced using a reflectivity database for multilayer crystals [8]. The two-dimensional image reproduces energy spectrum and the angular distribution of X-ray photons generated via nonlinear Compton scattering as shown in Fig. 3. (The square in Fig. 5 corresponds to the square in Fig. 3 and the upper half of the square in Fig. 4)

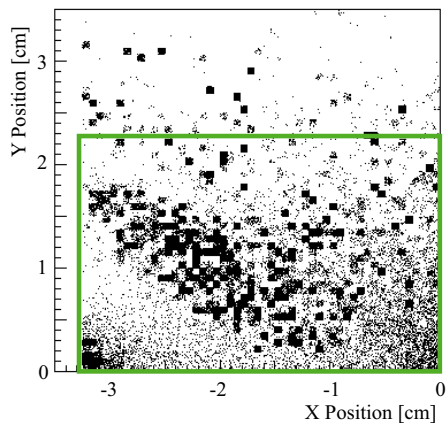


Figure 5: Simulated image of X-ray photons on the CCD detector. The photons are generated by CAIN for $a = 0.77$.

5 ACKNOWLEDGMENT

This study is supported by the Japan/US cooperation in the field of high energy physics and the US Department of Energy.

6 REFERENCES

- [1] P. Sprangle *et al.*, J. Appl. Phys. **72**, 5032 (1992).
- [2] S. Kashiwagi *et al.*, Nucl. Instr. Meth. A **455**, 36 (2000).
- [3] I. V. Pogorelsky *et al.*, Phys. Rev. **ST-AB 3**, 090702 (2000).
- [4] T. Kumita *et al.*, Proceedings of 21st ICFA beam Dynamics Workshop on laser-beam interactions, (2001).
- [5] T. J. Englert and E. A. Rinehart, Phys. Rev. A **28**, 1539 (1983).
- [6] C. Bula *et al.*, Phys. Rev. Lett. **76**, 3116 (1996).
- [7] P. Chen *et al.*, Nucl. Instr. Meth. A **355**, 107 (1995).
- [8] <http://www-cxro.lbl.gov/index.html>